Critical Parameters and Vapor Pressure Measurements of Hydrofluoroethers at High Temperatures

Masahiko Yasumoto,[†,§] Yasufu Yamada,[†] Jyunji Murata,[†] Shingo Urata,[†] and Katsuto Otake*[,‡,§]

Research Institute of Innovative Technology for the Earth, Hongo 2-40-17, Bunkyo-ku, Tokyo 113-0000, Japan, and Institute for Green Technology, and Research Center for Developing Fluorinated Greenhouse Gas Alternatives, National Institute of Advanced Industrial Science and Technology, Tsukuba Central 5, Higashi 1-1-1, Tsukuba, Ibaraki 305-8565, Japan

An apparatus was constructed for the measurement of critical parameters and vapor pressure at high temperatures. Its reliability was confirmed with two commercially available chlorofluorocarbons, HFC-134a (CF_3CH_2F) and HCFC-142b (CH_3CClF_2). Measured overall values fell well within the range of other reports. Attempts were made to measure the critical parameters of 21 newly synthesized hydrofluoroethers, that are potentially useful for dry-cleaning and have critical temperatures higher than 450 K. Before the measurements, great care was taken to remove traces of moisture from the samples. Among these new compounds, six were thermally unstable and four were rather unstable even after dehydration. The critical parameters of the remaining 11 were successfully obtained with good reproducibility. Their Antoine and Wagner parameters were also reported.

Introduction

Chlorofluorocarbons (CFCs) have been utilized extensively as refrigerants, blowing agents, and cleaning solvents due to their chemical stability and physical properties. However, their ozone layer depleting potential (ODP) makes them undesirable. Hence, their use, in accordance with the Kyoto Protocol (1997), is expected to be restricted soon. To meet the requirements of the agreement, it will be necessary to develop alternative substances that can satisfy the technical specifications of industry while reducing ODP.

Non-chlorine-containing fluorine compounds with heteroatoms such as O and N in their carbon chains (e.g. hydrofluoroethers (HFEs), hydrofluoroketones (HFKs), and hydrofluoroamines (HFAMs)) have lower ODPs since they are more easily decomposed by radical reactions occurring in the atmosphere.[1] For evaluation of these compounds in industrial systems, physical properties such as vapor pressure, critical temperature, critical pressure, and critical density are required.

In this article, we describe an apparatus for the visual determination of these properties, the experimental procedures, the results of validation tests, and the critical parameters of 11 thermally stable hydrofluoroethers out of 21 compounds with critical temperatures > 450 K.

The validity of the apparatus is illustrated by measurements of the critical parameters of HFC-134a (CF_3CH_2F) and HCFC-142b (CH_3CClF_2).

Experimental Section

Materials. The substances used in this study are summarized in Table 1 with sample code, molecular formula, purity, and normal boiling point.[5−7] They were all supplied by the Research Institute of Innovative Technology for the Earth (RITE). Their purities were monitored with a gas chromatograph (Hewlett-Packard, model HP-6890) equipped with a TCD detector.

A number of the substances measured in this study may be easily decomposed by impurities such as water. Therefore, we carried out a 12 h preliminary stability check using a simple apparatus comprised of a cylinder and a pressure gauge at temperatures 50 K higher than the estimated critical temperatures calculated by Joback's method.[8] Thermal decomposition was detected by a steep increase in pressure during the test, by change of the sample color before and after the test, and by gas chromatographic analysis. Substances judged to be thermally unstable were treated with molecular sieves 3A that had been dried at 620 K under vacuum for 2 h. Figure 1 shows the dehydration apparatus. After dehydration, the thermal stability was rechecked as described above. After confirmation that thermal reaction had not occurred, the critical parameters were measured with the optical cell.

Apparatus. Critical points of the new compounds were measured by observing the behavior of the meniscus at the vapor−liquid interface in an optical cell. The concept of the apparatus was similar to that discussed in previous work.[2−4] However, for the high temperature measurements with the small amounts of samples reported here, a newly designed rectangular shaped optical cell was used. For a precise visual observation of the critical point, simultaneous control of the sample mass in the optical vessel, or the density, and the precise control of temperature are essential. For the control of the density, a simple variable volume vessel was developed.

Figure 2 shows the experimental apparatus used in this study. It was composed of four main parts: a rectangularly shaped optical cell (A), two variable volume vessels (B), a differential null-pressure detector (C), and aluminum blocks (D, 2000 cm^3) that acted as thermal masses to

* Corresponding author. Phone: +81-29-861-4567 or +81-29-861-4819. Fax: +81-29-861-4567. E-mail: katsuto-otake@aist.go.jp.
† Research Institute of Innovative Technology for the Earth.
‡ Institute for Green Technology.
§ Research Center for Developing Fluorinated Greenhouse Gas Alternatives, National Institute of Advanced Industrial Science and Technology.

10.1021/je0201976 CCC: $25.00
Published on Web 10/03/2003

Table 1. Properties of Samples

sample code	molecular structure	CASRN	purity/%	T_b/K	name
HFE-245mf	$CF_3CH_2OCHF_2$	1885-48-9	99.8	302.15	2-difluoromethoxy-1,1,1-trifluoroethane
HFE-254pc	$CHF_2CF_2OCH_3$	425-88-7	99.9	310.34	2-methoxy-1,1,2,2-tetrafluoroethane
HFE-329mec	$CF_3CHFCF_2OCF_3$		99.8	331.15	3-trifluoromethoxy-1,1,1,2,3,3-hexafluoropropane
HFE-338mc-c	$CF_3CF_2OCF_2CH_2F$	142385-84-0	99.8	308.63	1,1,1,2,2-pentafluoro-2-(1,1,2-trifluoroethoxy)ethane
HFE-347pc-f	$CF_3CH_2OCF_2CHF_2$	406-78-0	99.99	329.37	1,1,2,2-tetrafluoro-1-(2,2,2-trifluoroethoxy)ethane
HFE-347mcf	$CF_3CF_2CH_2OCHF_2$	56860-81-2	99.7	319.09	3-difluoromethoxy-1,1,1,2,2-pentafluoropropane
HFE-356mf-f	$CF_3CH_2OCH_2CF_3$	333-36-8	99.8	336.91	1,1,1-trifluoro-2-(2,2,2-trifluoroethoxy)ethane
HFE-356mec	$CF_3CHFCF_2OCH_3$	382-34-3	99.4	327.47	3-methoxy-1,1,1,2,3,3-hexafluoropropane
HFE-356pcc	$CHF_2CF_2CF_2OCH_3$	10620-20-2	99.9	341.02	3-methoxy-1,1,2,2,3,3-hexafluoropropane
HFE-356pc-f	$CHF_2CF_2OCH_2CHF_2$	50807-77-7	99.8	352.13	1,1,2,2-tetrafluoro-2-(2,2-difluoroethoxy)ethane
HFE-356pcf	$CHF_2CF_2CH_2OCHF_2$	35042-99-0	99.9	348.6	3-difluoromethoxy-1,1,2,2-tetrafluoropropane
HFE-374pcf	$CHF_2CF_2CH_2OCH_3$	60598-17-6	99.1	347.5	3-methoxy-1,1,2,2-tetrafluoropropane
HFE-449mec-f	$CF_3CHFCF_2OCH_2CF_3$	993-95-3	99.8	345.87	1,1,1,2,3,3-hexafluoro-3-(2,2,2-trifluoroethoxy)propane
HFE-449mcf-c	$CF_3CF_2CH_2OCF_2CHF_2$	50807-74-4	99.8	343.4	1,1,1,2,2-pentafluoro-3-(1,1,2,2-tetrafluoroethoxy)-propane
HFE-458pcf-c	$CHF_2CF_2CH_2OCF_2CHF_2$	16627-68-2	99.7	366.32	1,1,2,2-tetrafluoro-3-(1,1,2,2-tetrafluoroethoxy)propane
HFE-458mecf	$CF_3CHFCF_2CH_2OCHF_2$	69948-46-5	99.8	361.55	4-difluoromethoxy-1,1,1,2,3,3-hexafluorobutane
HFE-467mccf	$CF_3CF_2CF_2CH_2OCH_3$	376-98-7	99.2	344.13	4-methoxy-1,1,1,2,2,3,3-heptafluorobutane
HFE-54-11mec-f	$CF_3CHFCF_2OCH_2CF_2CF_3$	1000-28-8	99.8	360.64	1,1,1,2,3,3-hexafluoro-3-(2,2,3,3,3-pentafluoropropoxy)-propane
HFE-55-10mec-fc	$CF_3CHFCF_2OCH_2CF_2CHF_2$	65064-78-0	99.8	379.07	1,1,1,2,3,3-hexafluoro-3-(2,2,3,3-tetrafluoropropoxy)-propane
HFE-569mccc	$CF_3CF_2CF_2CF_2OCH_2CH_3$	16370-05-4	99.8	350.04	4-ethoxy-1,1,1,2,2,3,3,4,4-nonafluorobutane
HFE-578pcccf	$CHF_2CF_2CF_2CF_2CH_2OCH_3$	77527-96-9	99.8	395.83	5-methoxy-1,1,2,2,3,3,4,4-octafluoropentane
HFC-134a	CF_3CH_2F	811-97-2	99.99	246.65	1,1,1,2-tetrafluoroethane
HCFC-142b	CH_3CClF_2	75-68-3	99.99	263.35	1-chloro-1,1-difluoroethane

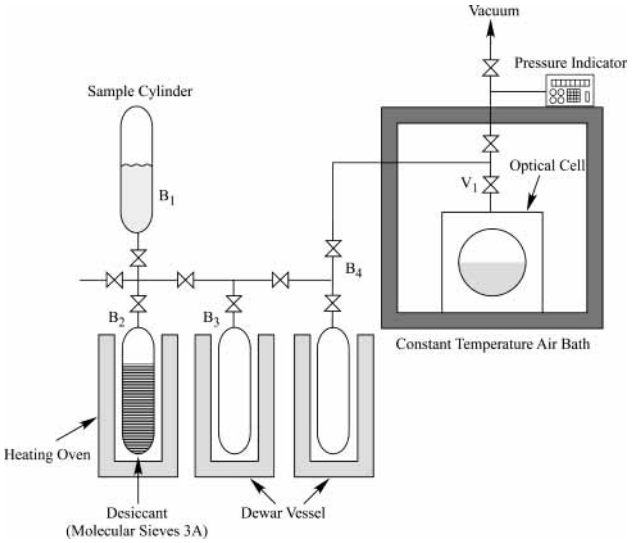

Figure 1. Schematic figure of the apparatus for the sample dehydration.

dampen temperature fluctuations. They were immersed in an oil bath (E: Chino, special model, with inner dimensions 600 mm × 400 mm × 650 mm) filled with silicon oil (Toshiba TSF451-100). The bath temperature was controlled to within ±3 mK in the range 400 to 450 K and to ±5 mK from 450 to 550 K using two electric heaters. These were equipped as follows (Figure 1): the main heater (G: 6 kW) was controlled by a Chino DB1230-000 (H) fitted with a Pt-100 Ω platinum resistance thermometer (I_1: Chino, R900-F25AT) and a thyristor regulator Chino JS-2050 (J), and the subheater (K: 2 kW) was controlled by a Chino DB1160-000 (L) equipped with a Pt-100 Ω platinum resistance thermometer (I_2: Chino, R900-F25AT) and an ASL ac bridge F300 (M_1). The flow inside the bath was optimized by fins (Q) to achieve optimal temperature control.

The temperature of samples was measured at three different points (optical cell, null-pressure detector, and variable volume vessel) with a Pt-100 Ω platinum resistance thermometer (N: Minco, model S7929) equipped with an ac bridge (M_2: ASL, model F300) calibrated on the basis of ITS-90 and two Pt-100 Ω platinum resistance thermometers (I_3, I_4: Chino, R900-F25AT) equipped with ac bridges (M_3, M_4: ASL, model F300). They were calibrated against the Minco thermometer described above. The accuracy of the thermometers was within ±10 mK according to the calibration by a supplier. Before experiments, all three thermometers were set at the same position of the optical cell to measure the differences between each other. It was smaller than 3 mK. Thus, we assumed that the accuracy in temperature measurements was less than ±10 mK.

Pressure was measured by the null-pressure detector (C: RUSKA, model 2439-800 and model 2461-800) equipped with quartz crystal pressure gauges (Paroscientific, Inc., model 2100A-101 for low pressure and model 31K-101 for high pressure) calibrated using a pneumatic dead weight pressure gauge that has the total uncertainty 0.005% in the high pressure range (7 MPa). Thus, we assumed that the uncertainty in the pressure is less than ±0.5 kPa.

Figure 3 shows the optical cell. It was made of 316 stainless steel and had two sapphire windows (25 mm × 10 mm) sealed with gold plated metal O-rings (INCONEL 718, 1.57 mm thick) and aluminum gaskets (1.3 mm thick). The inner volume of the optical cell with valve V_1 was 5.880 ± 0.002 cm^3, as determined by the mass of pure water to fill it completely under atmospheric conditions. The total system volume including piping and differential null-pressure detector was about 10 cm^3. The optical cell was connected to the two variable volume vessels and the differential null-pressure detector by a valve (V_1: Sno-Trik, model SS-445-FP-G). The central axis of these vessels and the detector were arranged at the same level.

Figure 4 is a schematic representation of the variable volume vessel that consists of metal bellows dismantled from a bellows valve (NUPRO, SS-4BG) and a body constructed in our own machine shop. The inner volume of the apparatus could be changed by turning the handle. We observed that the inner volume of the vessel changed 1 cm^3 with 10 turns of the handle. The critical density of the sample was calculated from the mass recovered from the optical cell and the inner volume of the optical cell. The mass was measured with an electronic balance

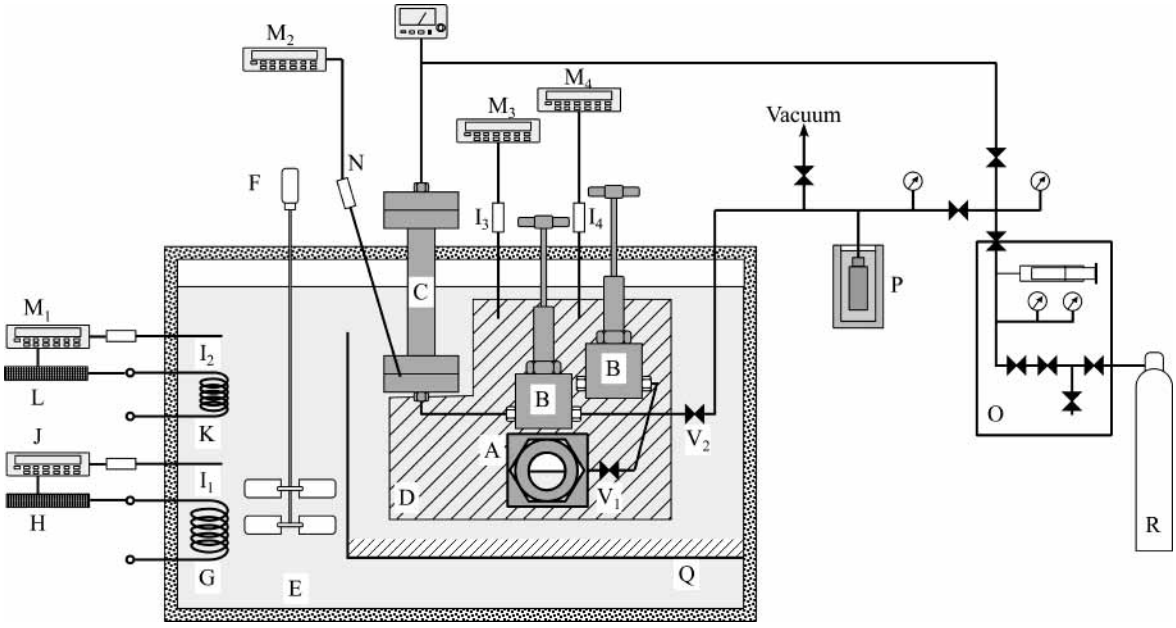

Figure 2. Schematic figure of the experimental apparatus: A, optical cell; B, variable volume vessel; C, differential null-pressure detector; D, aluminum blocks; E, constant temperature oil bath; F, impeller; G, main heater; H, main heater controller; I, platinum resistance thermometer; J, thyristor regulator; K, subheater; L, subheater controller; M, platinum resistance thermometer; N, platinum resistance thermometer; O, quartz crystal pressure detector; P, cold trap; Q, rectifier fin; R, N_2 cylinder.

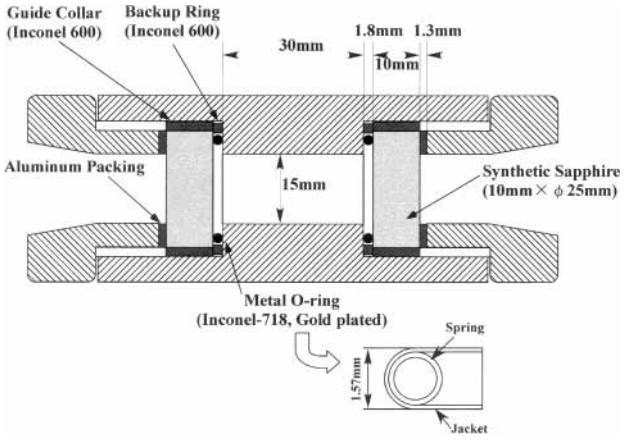

Figure 3. Schematic figure of the optical cell.

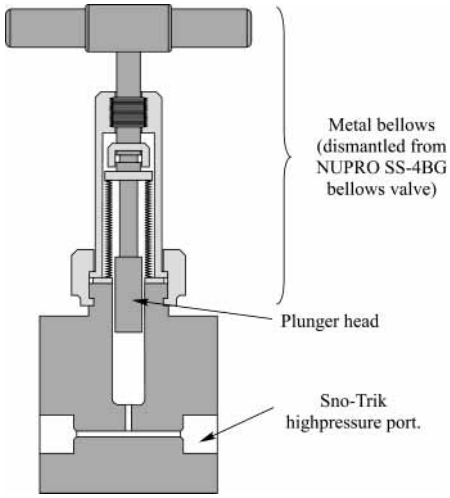

Figure 4. Schematic figure of the variable volume vessel.

(Mettler, model AT400) with an accuracy of 0.1 mg. As the sample mass was usually ~2.5 g, the inner volume of the optical cell was ~6 cm^3, and the minimum scale value of the electric balance was 0.1 mg, the error in the density measurements will be ±0.02 kg m^{-3}. Thus, we assumed the uncertainty in the density was less than ±1 kg m^{-3}.

Procedures. A sample was loaded to the optical cell from the dehydration apparatus shown in Figure 1. The cylinder (B_1) containing the undried sample was connected to the evacuated apparatus and the sample transferred to cylinder B_3 and then to cylinder B_4 under vacuum by using hot water and liquid nitrogen. Samples requiring dehydration were first transferred to the dehydration cylinder B_2 and then transferred to B_3 and B_4. The sample was then loaded into the optical cell situated in a constant temperature air bath at 233 K. The optical cell was disconnected from the apparatus at valve V_1 and then reconnected to the critical parameters' measurement apparatus shown in Figure 2. The loaded mass was measured with the AT400 electronic balance at the end of the experiment by trapping the samples in the cold trap (Figure 2, P). The critical density was calculated from the mass and the known inner volume of the optical cell.

After the optical cell was connected to the main apparatus (Figure 2), the remaining part of the apparatus was evacuated. After closing V_2 and opening V_1, the temperature was raised to a desired value in 10 K increments. For each change in the conditions, approximately 1 h of equilibration time was allowed before the temperature and vapor pressure were recorded. Since the experimental procedure is a static method, there is a distinct possibility that an equilibrium was not achieved during the vapor pressure measurements. To confirm that the vapor pressures measured are, in fact, the equilibrium values, the difference in the vapor pressure with and without stirring inside the optical cell was checked with CFC-134a. After the temperature and pressure were recorded, the position of the meniscus was controlled by the variable volume vessels (B) to be 1 to 2 mm above the center of the optical windows.

Near the critical temperature, when critical opalescence began to appear, the temperature increment was decreased to 10 mK. The phase change near the critical point is illustrated in Figure 5 by photos taken during the experi-

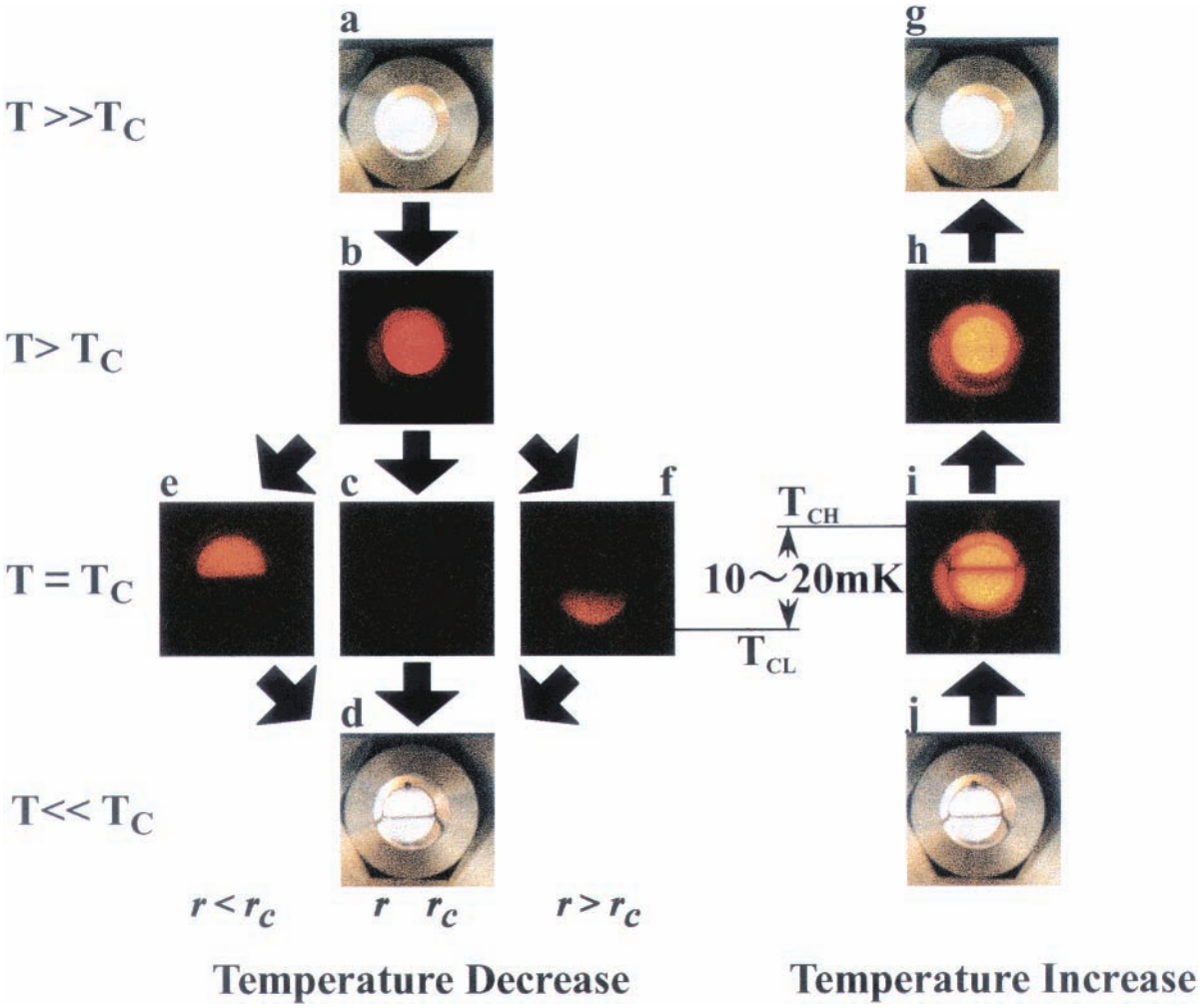

Figure 5. Schematic representation of the phase behavior near the critical temperature during the critical parameters' measurements.

ments. Note that, at the point of critical opalescence, insufficient light transmission caused photos taken at the critical temperature to become black (Figure 5c).

It was observed that as the temperature was decreased from supercritical to subcritical conditions, for density less than the critical density, the critical opalescence appeared in the liquid phase (Figure 5e). On the other hand, if the density was greater than the critical density, the critical opalescence appeared in the gas phase (Figure 5f). The density inside the optical cell was controlled by the variable volume vessels to give an equally strong critical opalescence in both the gas and the liquid phases. When the density was almost equal to the critical density, the critical opalescence could be observed in both liquid and gas phases (Figure 5b). The critical opalescence becomes most intense at the temperature T_{CL} (Figure 5c), and a further decrease in the temperature resulted in a clearly defined meniscus (Figure 5d). In most cases, the meniscus appeared upon condensation at 10 mK lower than T_{CL}. In contrast, on increasing the temperature, the disappearance of the meniscus and the appearance of the critical opalescence did not seem to be as clear-cut as those for the case of decreasing temperature. When the temperature was increased from the subcritical to supercritical, the interface between the gas and liquid phases appeared as a thick line (Figure 5i) at temperature T_{CH} and became thinner before disappearing (Figure 5h). For most experiments, T_{CH} was about 10 to 20 mK higher than T_{CL}. In this study, the numerical average of two T_{CL} values and two T_{CH} values was taken as the critical temperature. The critical pressure was calculated from a linear interpolation of the $p-T$ curve near the critical point.

After the critical parameters' measurements, V_1 was closed, and the sample inside the optical cell was trapped in the cold trap (Figure 2, P). The critical density was then determined from the mass of the sample and the known internal volume of the optical cell.

Measurements on thermally unstable samples were conducted twice. With dehydrated samples, approximate critical parameters were determined in a first experiment. Then, with a freshly dehydrated sample, determination of the critical parameters was conducted as quickly as possible to minimize unwanted reactions. For the case of the thermally stable samples, the approximate time required for the measurements was 10 to 30 h, depending on the critical temperature. On the other hand, for the case of the thermally unstable compounds, the approximate critical temperature was determined within 5 h in the first run. Then, the critical temperature was determined within another 5 or so hours in the second run.

Correlation. The vapor pressures were correlated using the Antoine equation,[8]

$$\log P = A - \frac{B}{T + C} \tag{1}$$

and the Wagner equation,[8]

Table 2. Critical Properties of Reference Samples

	first run				second run								
	temp decrease		temp increase		temp decrease		temp increase		avg				
sample code	T_c/K	P_c/MPa	T_c/K	P_c/MPa	T_c/K	P_c/MPa	T_c/K	P_C/MPa	T_c/K	σ	P_c/MPa	σ	ρ_c/kg·m^{-3}
HFC-134a	374.11	4.049	374.13	4.052	374.12	4.051	374.14	4.052	374.13	0.022	4.051	0.002	508
HCFC-142b	410.29	4.052	410.32	4.054	410.29	4.055	410.30	4.056	410.30	0.024	4.054	0.003	442

Table 3. Comparison of Critical Parameters of HFC-134a and HCFC-142b

compd	author	T_c/K	P_c/MPa	ρ_c/kg·m^{-3}	ref
HFC-134a	Maezawa et al.	374.30		508	9
(CF_3CH_2F)	Baehr et al.	374.18	4.058		10
	JAR&JFGA	374.30	4.065	511	11
	Stroem et al.	374.25	4.070		12
	Aoyama et al.	374.08		509	13
	Fujiwara et al.	374.07	4.050	509	14
	this work	374.13	4.053	508	
HCFC-142b	Mears et al.	410.25	4.119	435	15
(CH_3CClF_2)	Chae et al.	410.30		449	16
	Yada et al.	410.29	4.041		17
	Tanikawa et al.	410.29		446	18
	Stroem et al.	410.02	4.124		12
	this work	410.30	4.057	442	

$$\ln P_r = \frac{A(1 - T_r) + B(1 - T_r)^{1.5} + C(1 - T_r)^{2.5} + D(1 - T_r)^5}{T_r} \quad (2)$$

where P is the pressure in MPa and T is the temperature in K. T_r is the reduced temperature, given by $T_r = T/T_c$, P_r is the reduced pressure, given by $P_r = P/P_c$, T_c is the critical temperature, and P_c is the critical pressure.

Results and Discussion

Validation of the Apparatus. The apparatus and procedures were verified by performing measurements on the following compounds: HFC-134a and HCFC-142b, which have well-established literature values. The critical parameters of these compounds are shown in Table 2 together with their standard deviations. Table 3 provides a comparison of the values in this work with literature values.[9−21] The measured values fell within the range of other reports.

Figure 6 shows vapor pressures correlated with the Antoine and Wagner equations using data obtained in this study. The measured vapor pressures of these compounds also agreed well with the literature values. As can be seen from Figure 6a and d, there was no difference between data taken with and without stirring inside the optical cell.

Vapor Pressure and Critical Parameter Measurements. The measured critical parameters of stable compounds are given in Table 4 together with estimated values by Joback's method.[8] As shown by the standard deviations, reproducibility was good. The difference between experimental and estimated results showed that Joback's method predicted T_c to within ±2% and ρ_c and P_c to within ±11% and ±7%, respectively.

Tables 5 and 6 show the vapor pressures of these compounds and parameters for the Antoine and Wagner equations. Recently, Murata et al.[27] reported the normal boiling points of 50 hydrofluoroethers. In this report, some of the compounds used in our study were also used (HFE-449mec-f, -5410mec-fc, -5411mec-f, -458pcf-c, -578pc3f, -356pcf, -347pc-f, -356mf-f, -356pc-f, -356mec, -449mcf-c, -374pcf, -467mccf, and -569mccc). Figure 7 shows vapor

Table 4. Critical Properties of Thermally Stable Hydrofluoroethers

	experimental												
	first run				second run								
	temp decrease		temp increase		temp decrease		temp increase		avg		avg		
sample code	T_c/K	P_c/MPa	T_c/K	P_c/MPa	T_c/K	P_c/MPa	T_c/K	P_c/MPa	T_c/K	σ	P_c/MPa	σ	ρ_c/kg·m^{-3}
HFE-347pc-f	463.88	2.713	463.90	2.714	463.88	2.713	463.90	2.714	463.89	0.020	2.713	0.001	541
HFE-347mcf	455.07	2.770	455.11	2.773	455.09	2.771	455.12	2.775	455.10	0.038	2.773	0.004	576
HFE-356mf-f	476.29	2.782	476.31	2.784	476.29	2.782	476.33	2.784	476.31	0.033	2.783	0.002	500
HFE-356pc-f	501.07	3.088	501.08	3.092	501.07	3.089	501.10	3.092	501.08	0.024	3.090	0.004	520
HFE-374pcf	505.33	3.278	505.35	3.280	505.34	3.277	505.36	3.279	505.35	0.022	3.279	0.002	453
HFE-449mec-f	475.75	2.232	475.76	2.237	475.72	2.230	475.73	2.233	475.74	0.032	2.233	0.005	563
HFE-449mcf-c	472.99	2.243	473.04	2.245	473.00	2.243	473.02	2.245	473.01	0.038	2.244	0.002	550
HFE-458pcf-c	510.06	2.580	510.08	2.582	510.05	2.581	510.07	2.582	510.07	0.022	2.581	0.002	530
HFE-467mccf	481.50	2.379	481.57	2.383	481.51	2.379	481.57	2.383	481.54	0.065	2.381	0.004	497
HFE-54-11mec-f	486.47	1.949	486.49	1.952	486.47	1.949	486.49	1.951	486.48	0.020	1.950	0.003	567
HFE-569mccc	482.00	1.975	482.05	1.977	481.99	1.974	482.03	1.976	482.02	0.048	1.976	0.002	518

estimated by Joback's method[6]			deviation					
			critical temp		critical pressure		critical density	
T_c/K	P_c/MPa	ρ_c/kg·m^{-3}	ΔT_c/K	T_c(err)/%	ΔP_c/MPa	P_c(err)/%	$\Delta\rho_c$/kg·m^{-3}	ρ_c(err)/%
469.40	2.805	533	−5.51	−1.19	−0.092	−3.39	8	1.48
454.75	2.805	533	0.35	0.08	−0.032	−1.15	43	7.47
484.23	2.919	501	−7.92	−1.66	−0.136	−4.89	−1	−0.20
502.52	2.909	502	−1.44	−0.29	0.181	5.86	18	3.46
508.46	3.185	439	−3.11	−0.62	0.094	2.87	14	3.09
480.07	2.368	548	−4.33	−0.91	−0.135	−6.05	15	2.66
476.64	2.368	548	−3.63	−0.77	−0.124	−5.53	2	0.36
509.07	2.448	523	1.00	0.20	0.133	5.15	7	1.32
488.37	2.569	502	−6.83	−1.42	−0.188	−7.90	−5	−1.01
488.96	2.025	558	−2.48	−0.51	−0.075	−3.85	9	1.59
484.04	2.184	520	−2.02	−0.42	−0.208	−10.53	−2	−0.39

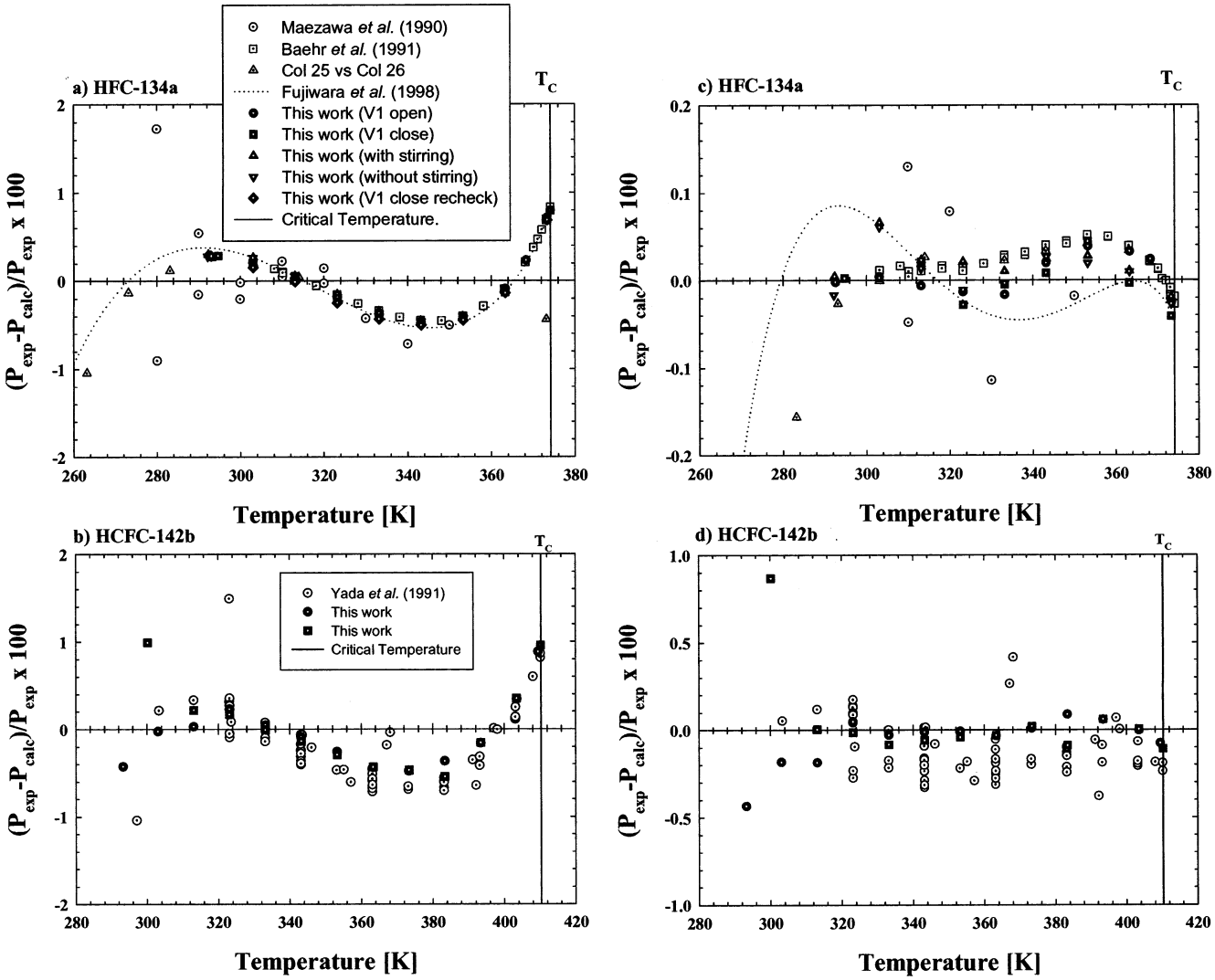

Figure 6. Vapor pressures of R-134a and R-142b correlated by the Antoine equation (a and c) and the Wagner equation (b and d).

pressures measured in this study together with the literature data. In this figure, results of the correlation were also indicated. Comparison with that data revealed that the vapor pressures obtained in our work were somewhat different from and generally higher than the literature values. This is presumably due to the effect of viscosity of the bath fluid used in this study. Because the experimental apparatus was optimized for measurements of critical parameters at high temperatures, the higher viscosity of the silicone oil at low temperature causes uncertainty in the temperature control.

Table 7 shows the measured critical parameters of partially unstable compounds together with their critical parameters estimated by Joback's method. In the table, the results of HFE-569mccc without dehydration are shown in order to demonstrate its importance. Although the dehydration improved the stability of the samples, all samples were still unstable compared with the compounds shown in Table 4. In this study, the maximum critical temperature measured was 546.1 K for HFE-578pc3f, and the maximum critical pressure was 3.47 MPa for HFE-245mf.

Table 8 shows the vapor pressures of some partially unstable compounds. Correlations with the Antoine and Wagner equations were difficult to make because of large deviations in both high and low temperature regions. The deviation at low temperatures could be attributed to the viscosity of the bath fluid, as described above, while those at high temperatures are probably the result of thermal decomposition. For example, in Table 7, the average critical temperature and pressure of HFE-5510-mec-fc are 516.2 K and 2.1763 MPa, respectively. On the other hand, in Table 8, the saturated vapor pressure of HFE-5510-mec-fc is 2.1763 MPa at 500.79 K, at about 16 K lower than the critical temperature. From Table 7, the tendency of the increase in critical pressure during the critical parameters' measurements is also clear. Since the correlation errors were relatively large, we have not tabulated the corresponding numerical values of the parameters here.

Compounds that could not be measured even after the dehydration are shown in Table 9 with critical parameters estimated with the Joback's method.[8] Even though the estimated critical temperatures were not very high, these compounds were unstable. In this context, it has been reported that HFEs having molecular structure groupings such as CHF_2OCH_2R, CH_2FOCH_2R, or $RCH_2OCF_2CH_2R'$ are unstable and that the existence of water, Cu, Fe, Al, and glass promotes their decomposition.[5] Tokuhashi et al.[22] reported that the order of the reaction rates with OH radicals is HFE-356pcf > HFE-347mcf > HFE-347pc-f. The attempted measurements in this work provide additional support for the instability of compounds with those structures. At the same time, the effectiveness of dehydration was confirmed, as this enabled the critical parameters for HFE-347mcf to be measured.

Table 5. Saturated Vapor Pressure of Thermally Stable Hydrofluoroethers

T	P_v(exp)	P_v(Antoine eq)	dev	P_v(Wagner eq)	dev	T	P_v(exp)	P_v(Antoine eq)	dev	P_v(Wagner eq)	dev
K	MPa	MPa	%	MPa	%	K	MPa	MPa	%	MPa	%
(a) HFE-347pc-f ($CHF_2CF_2OCH_2CF_3$)											
297.29	0.0278	0.0277	0.14	0.0277	0.12	402.83	0.8212	0.8253	−0.50	0.8218	−0.07
313.67	0.0557	0.0559	−0.40	0.0559	−0.37	413.90	1.0462	1.0526	−0.61	1.0460	0.01
322.82	0.0799	0.0798	0.11	0.0799	0.06	422.92	1.2609	1.2698	−0.70	1.2606	0.03
332.69	0.1145	0.1143	0.24	0.1144	0.10	432.91	1.5364	1.5472	−0.70	1.5358	0.04
342.88	0.1620	0.1614	0.38	0.1617	0.17	442.98	1.8593	1.8693	−0.54	1.8584	0.05
352.74	0.2212	0.2205	0.32	0.2210	0.09	452.95	2.2310	2.2335	−0.11	2.2301	0.04
362.70	0.2968	0.2964	0.16	0.2970	−0.04	462.99	2.6685	2.6492	0.72	2.6693	−0.03
372.69	0.3914	0.3915	−0.04	0.3919	−0.14	463.89	2.7133	2.6890	0.90	2.7130	0.01
382.81	0.5106	0.5105	0.03	0.5102	0.08	463.94	2.7158	2.6912	0.90		
392.83	0.6517	0.6537	−0.32	0.6522	−0.09						
(b) HFE-347mcf ($CF_3CF_2CH_2OCHF_2$)											
298.42	0.0442	0.0445	−0.57	0.0443	−0.08	392.82	0.8077	0.8112	−0.44	0.8077	−0.01
322.49	0.1115	0.1111	0.40	0.1114	0.12	402.86	1.0063	1.0145	−0.82	1.0077	−0.15
332.63	0.1572	0.1565	0.48	0.1571	0.05	412.90	1.2445	1.2541	−0.77	1.2437	0.06
342.70	0.2166	0.2152	0.67	0.2162	0.19	422.93	1.5249	1.5335	−0.56	1.5203	0.31
352.65	0.2907	0.2892	0.50	0.2904	0.08	432.96	1.8584	1.8567	0.09	1.8436	0.79
362.73	0.3841	0.3834	0.20	0.3845	−0.09	442.98	2.2033	2.2272	−1.08	2.2216	−0.83
372.78	0.4981	0.4996	−0.30	0.4999	−0.37	454.99	2.7690	2.7391	1.08	2.7673	0.06
382.79	0.6375	0.6408	−0.51	0.6397	−0.33	455.27	2.7964	2.7520	1.59		
(c) HFE-356mf-f ($CF_3CH_2OCH_2CF_3$)											
293.40	0.0180	0.0180	0.13	0.0181	−0.07	343.24	0.1292	0.1290	0.10	0.1291	0.07
293.59	0.0182	0.0182	0.34	0.0182	0.14	343.24	0.1292	0.1290	0.10	0.1291	0.07
303.09	0.0279	0.0280	−0.15	0.0280	−0.07	353.27	0.1783	0.1779	0.19	0.1781	0.10
303.12	0.0280	0.0280	0.05	0.0280	0.13	353.28	0.1783	0.1780	0.18	0.1781	0.08
313.12	0.0426	0.0427	−0.42	0.0427	−0.26	363.31	0.2411	0.2406	0.23	0.2409	0.11
313.14	0.0428	0.0428	−0.04	0.0427	0.12	363.31	0.2411	0.2406	0.22	0.2409	0.10
323.15	0.0633	0.0634	−0.20	0.0633	−0.06	373.34	0.3200	0.3195	0.15	0.3198	0.06
323.17	0.0634	0.0634	−0.10	0.0633	0.04	373.35	0.3201	0.3195	0.17	0.3198	0.09
333.20	0.0913	0.0915	−0.26	0.0915	−0.20	383.38	0.4174	0.4174	0.00	0.4174	−0.01
333.20	0.0914	0.0916	−0.17	0.0915	−0.11	383.38	0.4173	0.4174	−0.03	0.4174	−0.04
338.22	0.1090	0.1090	−0.03	0.1090	−0.02	393.43	0.5362	0.5373	−0.20	0.5366	−0.07
338.22	0.1090	0.1090	−0.05	0.1090	−0.04	393.43	0.5363	0.5374	−0.19	0.5367	−0.06
(d) HFE-356pc-f ($CHF_2CF_2OCH_2CHF_2$)											
300.91	0.0128	0.0128	0.74	0.0128	0.33	422.92	0.7239	0.7270	−0.42	0.7256	−0.24
322.65	0.0339	0.0342	−0.89	0.0341	−0.64	432.95	0.8982	0.9033	−0.56	0.8999	−0.20
332.67	0.0508	0.0513	−0.90	0.0511	−0.67	442.97	1.1024	1.1096	−0.66	1.1037	−0.12
342.69	0.0750	0.0746	0.52	0.0745	0.64	453.00	1.3416	1.3494	−0.58	1.3405	0.09
352.73	0.1061	0.1061	0.05	0.1061	0.03	463.02	1.6154	1.6252	−0.61	1.6137	0.10
362.73	0.1475	0.1471	0.24	0.1473	0.10	473.05	1.9310	1.9403	−0.48	1.9285	0.13
372.78	0.2025	0.2003	1.09	0.2007	0.87	482.09	2.2567	2.2604	−0.16	2.2523	0.20
382.80	0.2681	0.2674	0.27	0.2681	0.02	491.90	2.6581	2.6488	0.35	2.6541	0.15
392.83	0.3514	0.3510	0.10	0.3518	−0.12	497.81	2.9327	2.9045	0.96	2.9265	0.21
402.87	0.4535	0.4538	−0.08	0.4544	−0.20	501.30	3.1016	3.0634	1.23		
412.89	0.5767	0.5781	−0.24	0.5780	−0.22						
(e) HFE-374pcf ($CHF_2CF_2CH_2OCH_3$)											
342.68	0.0848	0.0859	−1.21	0.0852	−0.42	432.93	0.9348	0.9392	−0.48	0.9358	−0.11
347.65	0.1012	0.1017	−0.45	0.1013	−0.10	442.97	1.1381	1.1459	−0.69	1.1389	−0.07
352.72	0.1205	0.1201	0.34	0.1201	0.35	452.99	1.3735	1.3838	−0.75	1.3729	0.04
362.75	0.1661	0.1645	1.00	0.1652	0.54	463.01	1.6428	1.6560	−0.80	1.6417	0.07
372.76	0.2227	0.2207	0.88	0.2223	0.19	473.02	1.9520	1.9648	−0.66	1.9489	0.16
382.79	0.2934	0.2913	0.72	0.2935	−0.01	480.13	2.1973	2.2080	−0.49	2.1931	0.19
392.80	0.3799	0.3781	0.48	0.3805	−0.16	489.95	2.5733	2.5781	−0.19	2.5708	0.10
402.80	0.4843	0.4835	0.16	0.4857	−0.30	499.77	3.0059	2.9901	0.53	3.0029	0.10
412.88	0.6107	0.6112	−0.08	0.6123	−0.28	505.06	3.2628	3.2302	1.00	3.2639	−0.03
422.91	0.7588	0.7621	−0.42	0.7614	−0.34	505.35	3.2789	3.2438	1.07	3.2790	0.00
(f) HFE-449mec-f ($CF_3CHFCF_2OCH_2CF_3$)											
302.76	0.0187	0.0190	−1.32	0.0189	−0.81	402.89	0.5212	0.5235	−0.44	0.5222	−0.19
312.63	0.0296	0.0294	0.63	0.0294	0.86	412.92	0.6573	0.6601	−0.42	0.6567	0.10
322.65	0.0446	0.0445	0.31	0.0445	0.26	422.94	0.8143	0.8219	−0.93	0.8157	−0.17
332.64	0.0657	0.0652	0.73	0.0654	0.42	432.97	1.0044	1.0120	−0.76	1.0028	0.16
342.72	0.0939	0.0935	0.49	0.0939	0.01	443.00	1.2256	1.2329	−0.59	1.2216	0.33
352.73	0.1310	0.1305	0.37	0.1313	−0.20	453.02	1.4803	1.4871	−0.46	1.4767	0.25
362.77	0.1791	0.1786	0.27	0.1796	−0.29	463.04	1.7785	1.7776	0.05	1.7748	0.21
372.79	0.2397	0.2395	0.07	0.2406	−0.39	473.06	2.1250	2.1070	0.85	2.1269	−0.09
382.83	0.3159	0.3158	0.02	0.3167	−0.25	475.79	2.2361	2.2038	1.45		
392.84	0.4080	0.4094	−0.35	0.4095	−0.38						
(g) HFE-449mcf-c ($CF_3CF_2CH_2OCF_2CHF_2$)											
299.64	0.0177	0.0175	0.62	0.0176	0.08	412.89	0.7000	0.7003	−0.05	0.6996	0.05
332.69	0.0698	0.0703	−0.71	0.0701	−0.46	422.91	0.8686	0.8696	−0.12	0.8685	0.01
337.70	0.0840	0.0844	−0.37	0.0842	−0.15	432.95	1.0661	1.0678	−0.16	1.0670	−0.08
342.70	0.1003	0.1005	−0.19	0.1003	0.00	442.97	1.2980	1.2968	0.10	1.2978	0.02

Table 5 (Continued)

T	P_v(exp)	P_v(Antoine eq)	dev	P_v(Wagner eq)	dev	T	P_v(exp)	P_v(Antoine eq)	dev	P_v(Wagner eq)	dev
K	MPa	MPa	%	MPa	%	K	MPa	MPa	%	MPa	%
(g) HFE-449mcf-c ($CF_3CF_2CH_2OCF_2CHF_2$) (Continued)											
347.73	0.1192	0.1192	0.07	0.1190	0.21	447.99	1.4274	1.4240	0.23	1.4272	0.01
352.74	0.1406	0.1404	0.18	0.1402	0.28	453.00	1.5673	1.5598	0.48	1.5663	0.06
362.76	0.1922	0.1917	0.27	0.1916	0.29	458.02	1.7184	1.7049	0.79	1.7166	0.10
372.78	0.2568	0.2566	0.07	0.2567	0.05	464.03	1.9141	1.8910	1.21	1.9124	0.08
382.81	0.3376	0.3376	0.01	0.3377	−0.01	468.05	2.0552	2.0233	1.55	2.0543	0.04
392.84	0.4363	0.4369	−0.14	0.4369	−0.13	473.08	2.2466	2.1979	2.17		
402.86	0.5551	0.5569	−0.33	0.5566	−0.27						
(h) HFE-458pcf-c ($CHF_2CF_2CH_2OCF_2CHF_2$)											
322.65	0.0209	0.0209	−0.06	0.0208	0.22	432.96	0.6283	0.6262	0.34	0.6264	0.30
332.65	0.0316	0.0318	−0.57	0.0317	−0.28	442.99	0.7739	0.7756	−0.21	0.7744	−0.06
342.71	0.0468	0.0470	−0.45	0.0469	−0.28	453.01	0.9469	0.9503	−0.35	0.9470	−0.01
352.73	0.0679	0.0676	0.33	0.0676	0.33	463.24	1.1514	1.1574	−0.52	1.1517	−0.02
362.77	0.0954	0.0952	0.28	0.0953	0.09	473.06	1.3785	1.3859	−0.54	1.3783	0.01
372.77	0.1313	0.1309	0.33	0.1313	−0.02	481.12	1.5910	1.5971	−0.38	1.5890	0.13
382.81	0.1773	0.1768	0.29	0.1776	−0.16	491.90	1.9076	1.9149	−0.38	1.9103	−0.14
402.88	0.3081	0.3063	0.60	0.3077	0.14	501.73	2.2452	2.2425	0.12	2.2493	−0.18
412.91	0.3954	0.3939	0.37	0.3954	0.00	509.65	2.5525	2.5342	0.71	2.5629	−0.41
422.94	0.5002	0.4998	0.08	0.5010	−0.14						
(i) HFE-467mccf ($CF_3CF_2CF_2CH_2OCH_3$)											
291.65	0.0121	0.0124	−3.04	0.0121	−0.49	402.88	0.5313	0.5351	−0.71	0.4216	−0.47
302.31	0.0204	0.0206	−0.98	0.0204	−0.04	412.90	0.6643	0.6703	−0.90	0.5331	−0.34
312.43	0.0323	0.0320	0.73	0.0321	0.63	422.92	0.8203	0.8294	−1.11	0.6653	−0.16
322.64	0.0489	0.0484	1.19	0.0487	0.40	432.95	1.0046	1.0152	−1.05	0.8208	−0.06
332.66	0.0715	0.0704	1.57	0.0712	0.41	442.98	1.2164	1.2297	−1.09	1.0025	0.21
337.71	0.0854	0.0842	1.46	0.0852	0.20	453.00	1.4629	1.4751	−0.84	1.2133	0.25
342.70	0.1012	0.0999	1.33	0.1012	0.03	463.01	1.7461	1.7536	−0.43	1.4567	0.42
347.73	0.1192	0.1179	1.10	0.1195	−0.21	473.05	2.0711	2.0685	0.12	1.7373	0.50
362.74	0.1892	0.1877	0.77	0.0121	−0.49	478.44	2.2663	2.2531	0.58	2.0626	0.41
372.75	0.2502	0.2498	0.15	0.1897	−0.30	481.50	2.3825	2.3629	0.82	2.2591	0.32
382.82	0.3266	0.3272	−0.21	0.2517	−0.63	481.66	2.3891	2.3688	0.85		
392.85	0.4196	0.4215	−0.45	0.3286	−0.62						
(j) HFE-54-11mec-f ($CF_3CHFCF_2OCH_2CF_2CF_3$)											
312.48	0.0147	0.0147	0.23	0.0147	0.08	422.79	0.5754	0.5797	−0.76	0.5781	−0.47
342.64	0.0548	0.0549	−0.18	0.0548	0.06	432.96	0.7171	0.7232	−0.86	0.7192	−0.30
352.72	0.0791	0.0799	−0.90	0.0798	−0.87	443.00	0.8819	0.8885	−0.75	0.8817	0.02
362.78	0.1131	0.1129	0.14	0.1131	−0.03	453.00	1.0674	1.0786	−1.06	1.0694	−0.19
372.77	0.1570	0.1555	0.97	0.1560	0.66	461.47	1.2553	1.2609	−0.45	1.2511	0.33
382.71	0.2117	0.2092	1.18	0.2100	0.82	473.07	1.5487	1.5443	0.28	1.5399	0.57
402.89	0.3606	0.3610	−0.11	0.3616	−0.29	483.09	1.8428	1.8223	1.11	1.8361	0.36
412.90	0.4607	0.4614	−0.16	0.4613	−0.12	486.67	1.9543	1.9295	1.27	0.3616	−0.29
(k) HFE-569mccc ($CF_3CF_2CF_2CF_2OCH_2CH_3$)											
309.21	0.0225	0.0224	0.26	0.0224	0.17	402.87	0.4433	0.4408	0.55	0.4423	0.21
332.68	0.0570	0.0571	−0.22	0.0569	0.15	412.66	0.5534	0.5500	0.61	0.5513	0.38
342.71	0.0807	0.0813	−0.73	0.0811	−0.47	422.65	0.6848	0.6809	0.56	0.6816	0.47
347.73	0.0954	0.0961	−0.76	0.0960	−0.59	432.89	0.8353	0.8377	−0.28	0.8370	−0.20
382.82	0.2719	0.2689	1.12	0.2699	0.77	443.20	1.0116	1.0206	−0.90	1.0181	−0.64
392.84	0.3492	0.3468	0.69	0.3481	0.31	453.14	1.2129	1.2228	−0.82	1.2184	−0.45
						473.46	1.7207	1.7227	−0.12	1.7194	0.07

Table 6. Numerical Values of the Coefficients for Eqs 1 and 2 and Average Absolute Deviation (AAD)

	temp range/K		parameters for the Antoine equation (eq 1)				parameters for the Wagner equation (eq 2)				
	T_{min}	T_{max}	A	B	C	AAD/%	A	B	C	D	AAD/%
HFE-347pc-f	297	T_c	3.429 38	1254.314 57	−45.756 30	0.41	−8.447 73	2.288 45	−5.513 01	5.018 66	0.08
HFE-347mcf	298	T_c	3.569 12	1348.324 85	−24.423 19	0.63	−8.512 65	2.640 05	−4.848 33	4.443 41	0.13
HFE-356mf-f	293	T_c	3.514 05	1349.732 48	−36.714 41	0.17	−8.250 61	1.817 95	−4.482 79	5.051 92	0.09
HFE-356pc-f	300	T_c	3.440 63	1326.762 88	−52.223 50	0.53	−8.477 18	2.533 83	−5.945 45	5.091 79	0.25
HFE-374pcf	342	T_c	3.384 64	1319.064 83	−46.319 57	0.62	−8.107 14	2.224 88	−4.199 43	−7.291 90	0.18
HFE-449mec-f	302	T_c	3.378 75	1297.404 74	−48.391 39	0.55	−8.858 00	3.096 44	−6.555 84	4.232 29	0.30
HFE-449mcf-c	299	T_c	3.283 01	1225.170 65	−56.498 65	0.47	−8.568 11	2.337 75	−5.981 86	5.801 51	0.12
HFE-458pcf-c	322	T_c	3.420 67	1380.937 07	−51.904 60	0.36	−8.589 76	2.567 45	−6.151 09	5.898 47	0.15
HFE-467mccf	291	T_c	3.255 94	1239.392 85	−51.527 67	0.98	−8.291 09	2.288 43	−4.457 46	−6.290 31	0.33
HFE-54-11mec-f	312	T_c	3.035 39	1100.703 66	−86.405 20	0.65	−8.865 79	3.500 59	−10.022 49	8.442 53	0.34
HFE-569mccc	300	T_c	3.148 08	1216.710 90	−55.615 09	0.59	−7.889 98	1.570 25	−5.567 42	7.915 90	0.38

Critical temperature measurements of thermally unstable compounds have been conducted by Mogollon et al.,[23] Smith et al.,[24] Rosenthal and Teja,[25] and Quadri et al.[26] in the temperature range from 550 to 690 K by a sealed-tube method. In these reports, the uncertainty in temperature was ±0.1 to 0.2 K[23] and ±0.4 to 0.6 K,[24] and a slow variation of the T_c with time was noted. In our study, using a precise constant temperature oil bath, the uncertainty

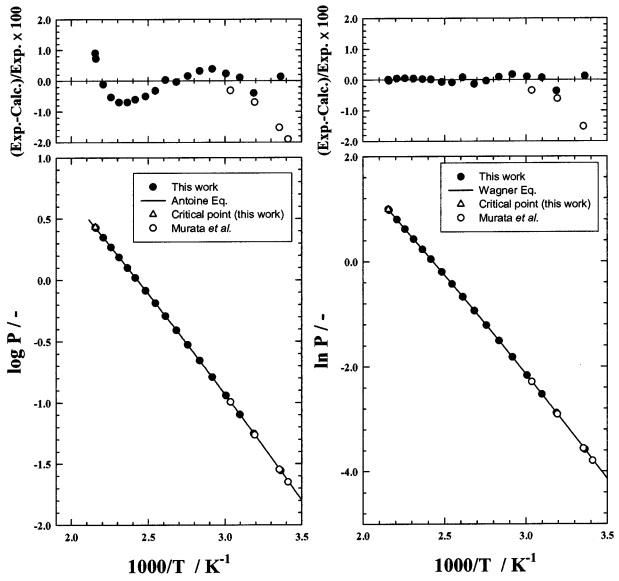

(a) HFE-347pc-f

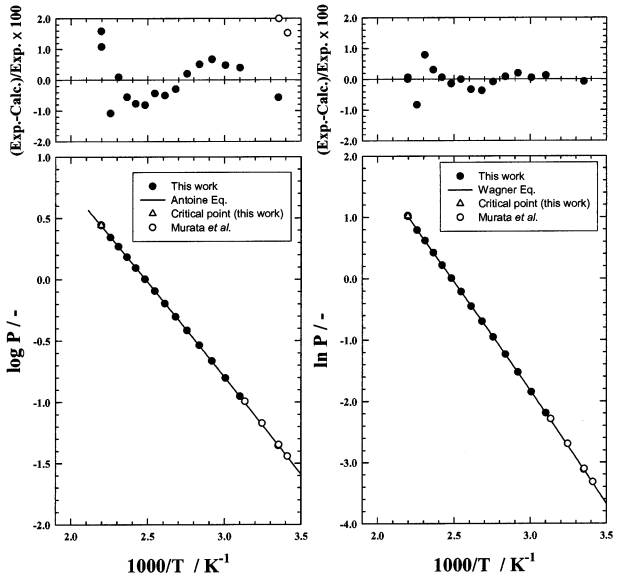

(b) HFE-347mcf

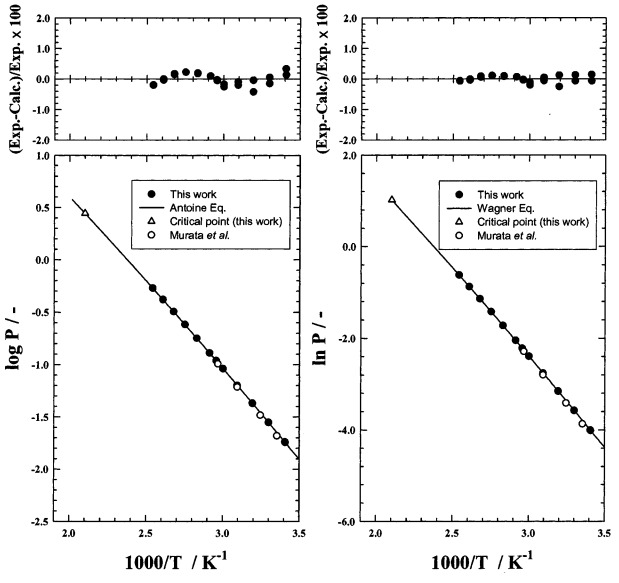

(c) HFE-356mf-f

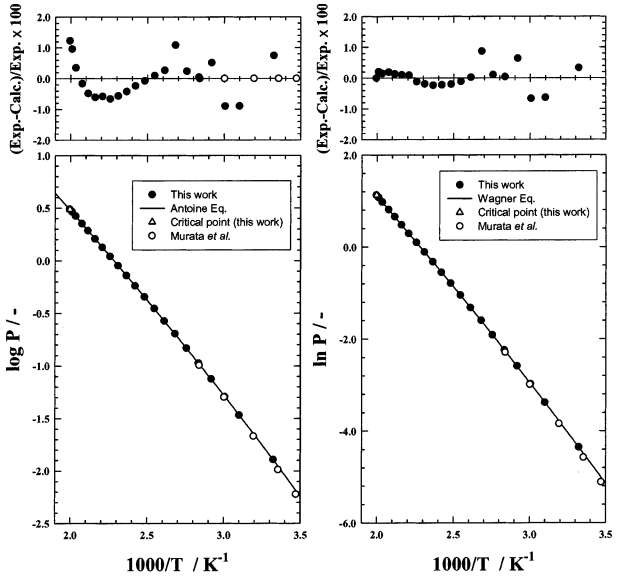

(d) HFE-356pc-f

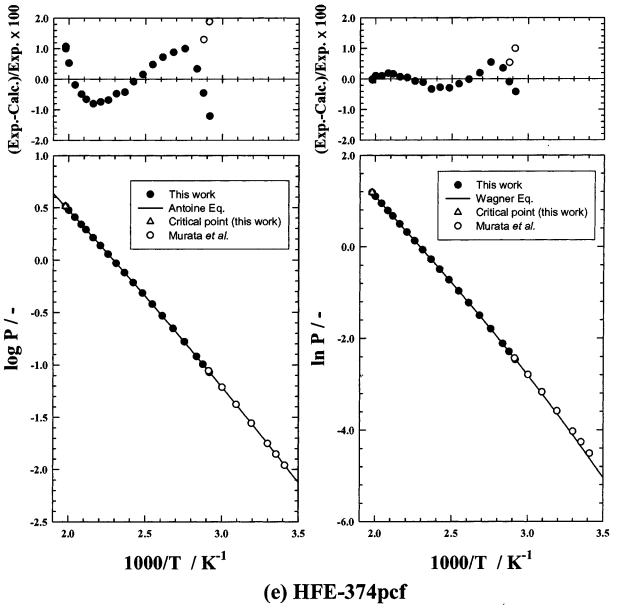

(e) HFE-374pcf

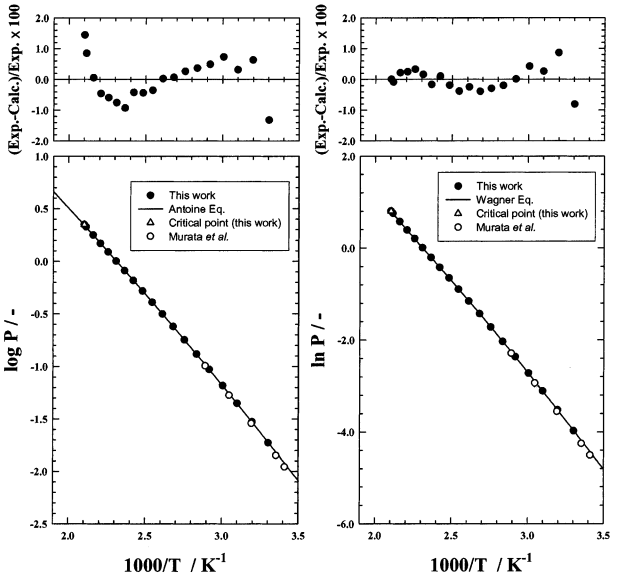

(f) HFE-449mec-f

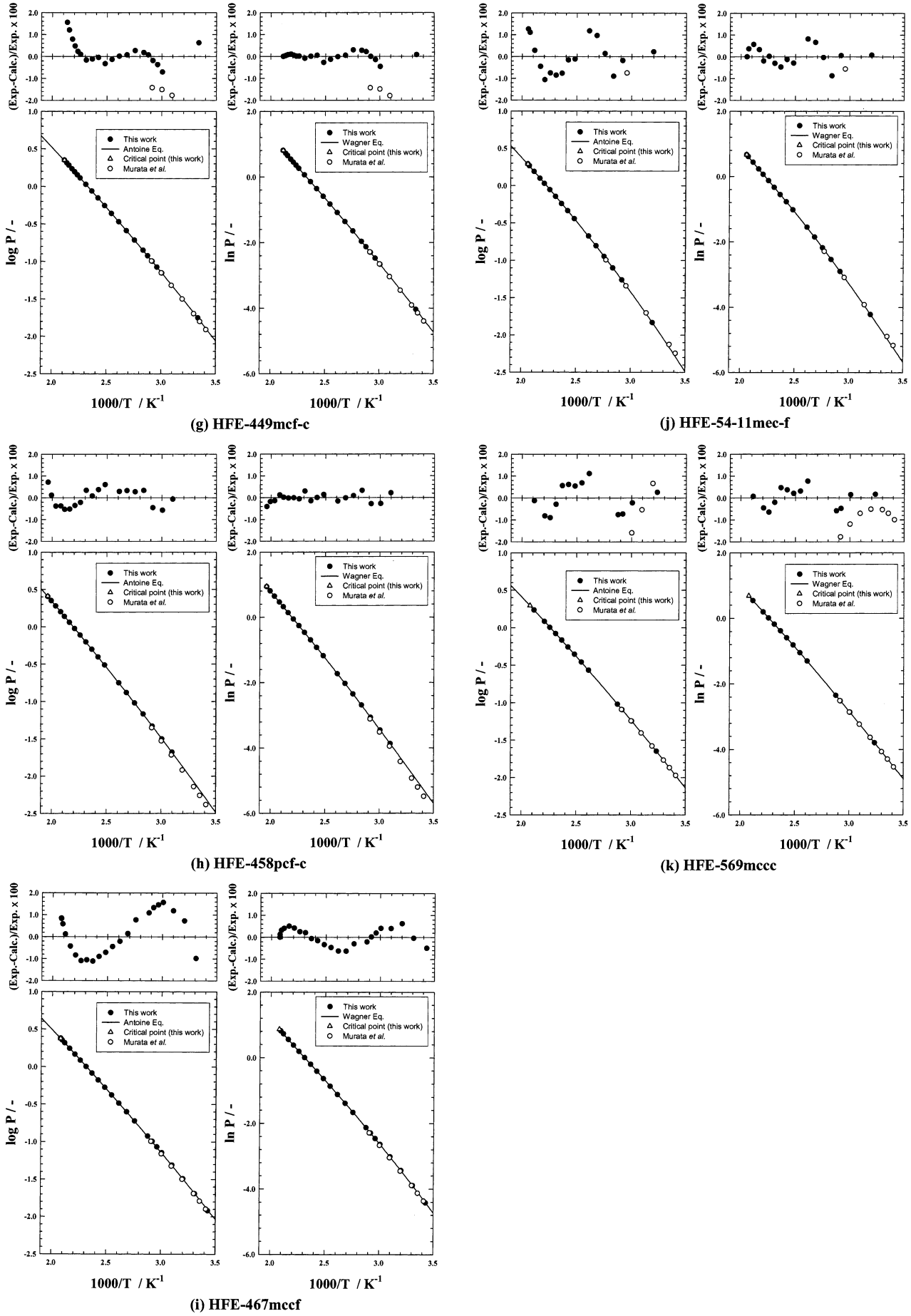

Figure 7. Vapor pressures of the thermally stable compounds.

Table 7. Critical Properties of Partially Unstable Hydrofluoroethers

	experimental											
	first run				second run							
	temp decrease		temp increase		temp decrease		temp increase		estimated by Joback's method[6]			
sample code	T_c/K	P_c/MPa	T_c/K	P_c/MPa	T_c/K	P_c/MPa	T_c/K	P_c/MPa	T_c/K	P_c/MPa	ρ_c/kg·m^{-3}	note
HFE-245mf	444.85	3.456	444.90	3.458	444.89	3.462	444.92	3.467	443.53	3.376	532	*a*
HFE-356pcc			486.98	3.032	487.03	3.192			493.77	2.944	565	*a*
HFE-569mccc			473.46	1.721			473.80	1.796				*b*
	482.00	1.975	482.05	1.977	481.99	1.974	482.03	1.976	484.04	2.184	518	*c*
HFE-578pcccf			545.58	2.603								*b*
	546.08	2.390	546.13	2.393	546.12	2.530	546.19	2.535	548.01	2.255	450	*a*
HFE-55-10mec-fc	516.20	2.171	516.22	2.174	516.25	2.184			514.50	2.089	560	*a*

[a] With dehydration; decomposition occurred during the second run. [b] Without dehydration; shown for comparison. [c] With dehydration; successfully measured after the dehydration; shown for comparison.

Table 8. Saturated Vapor Pressure of Relatively Unstable Hydrofluoroethers

T/K	*P*/MPa	*T*/K	*P*/MPa	*T*/K	*P*/MPa	*T*/K	*P*/MPa
HFE-245mf							
294.35	0.0723	323.16	0.2078	373.34	0.8230	423.52	2.3342
298.14	0.0843	333.19	0.2846	383.37	1.0319	433.56	2.7985
300.20	0.0915	343.23	0.3812	393.42	1.2826	443.56	3.3392
303.14	0.1028	353.26	0.5009	403.45	1.5758		
313.12	0.1481	363.30	0.6468	413.47	1.9195		
HFE-356pcc							
301.90	0.0224	342.69	0.1092	392.84	0.4588	442.97	1.3337
312.59	0.0350	352.73	0.1511	402.87	0.5811	452.99	1.6051
322.63	0.0529	362.74	0.2049	412.87	0.7262	463.02	1.9218
332.69	0.0770	372.78	0.2734	422.91	0.8988	473.04	2.2764
337.67	0.0921	382.81	0.3574	432.94	1.1007	480.12	2.5629
HFE-578pc3f							
301.49	0.0023	372.79	0.0743	442.97	0.4828	1.6159	512.54
312.42	0.0040	382.81	0.1068	452.99	0.5858	1.8735	522.34
322.54	0.0069	392.83	0.1471	463.00	0.7107	2.1687	532.17
332.62	0.0112	402.86	0.1938	473.04	0.8495	2.4719	541.94
342.67	0.0181	412.89	0.2504	483.07	1.0069	2.6025	545.63
352.72	0.0291	422.92	0.3201	492.89	1.1849		
362.75	0.0480	432.94	0.3957	502.72	1.3859		
HFE-5510mec-fc							
485.28	0.0062	352.75	0.0885	412.92	0.4691	473.08	1.4844
302.65	0.0125	362.72	0.1299	422.94	0.5818	481.14	1.7454
312.63	0.0198	372.80	0.1753	432.97	0.7155	490.97	2.0480
322.62	0.0309	382.83	0.2290	443.00	0.8709	499.97	2.1378
332.69	0.0458	392.86	0.2948	453.03	1.0495	500.79	2.1763
342.69	0.0629	402.89	0.3747	463.06	1.2529		

Table 9. Unstable Hydrofluoroethers

	estimated critical parameters by Joback's method[8]		
sample code	T_c/K	P_c/MPa	ρ_c/kg·m^{-3}
HFE-254pc	463.70	3.560	478
HFE-329mec	467.48	2.606	589
HFE-338mc-c	439.25	2.707	561
HFE-356mec	474.15	2.944	509
HFE-356pcf	497.48	2.909	502
HFE-458mecf	502.44	2.448	523

in the temperature measurement was successfully suppressed to <10 mK in the temperature range below 550 K. Possible reactions were suppressed by dehydration.

Conclusions

Precise measurements of the critical temperature, pressure, and density of 21 fluoroethers, potentially useful for dry-cleaning, have been conducted. Among them, six were found to be thermally unstable and four were rather unstable, especially in the presence of moisture. The critical parameters of the remaining eleven compounds were successfully determined. The Antoine and Wagner parameters are also reported. Removal of traces of water was found to be essential for the success of the procedure. Joback's method was found to be applicable for the prediction of critical temperature, with less accuracy being obtained for the critical pressure and density.

Acknowledgment

We thank members of RITE in Tsukuba for their help and our technician, Mr. Aso, for his help in the construction of the optical cell and the variable volume vessels. We are grateful to Dr. R. L. Smith, Jr., for useful discussions.

Literature Cited

(1) Ravishankara, A. R.; Tunipseed, A. A.; Jensen, N. R.; Barone, S.; Mills, M.; Howard, C. J.; Solomon, S. Do Hydrofluorocarbons Destroy Stratospheric Ozone? *Science* **1994**, *263*, 71.

(2) Sako, T.; Sato, M.; Nakazawa, N.; Oowa M.; Yasumoto, M.; Ito, H.; Yamashita, S. Critical parameters of fluorinated ethers. *J. Chem. Eng. Data* **1996**, *41*, 802−805.

(3) Sako, T.; Yasumoto, M.; Sato, M.; Kitao, O.; Ishiguro, K.; Kato, M. Measurement of critical parameters of fluorinated ethers and amines. *Fluid Phase Equilib.* **1998**, *144*, 113−117.

(4) Sako, T.; Yasumoto, M.; Nakazawa, N.; Kamizawa, C. Critical Parameters and Normal Boiling Temperatures of Five Fluorinated Ethers and Two Fluorinated Ketones. *J. Chem. Eng. Data* **2001**, *46*, 1078.

(5) Research Institute of Innovative Technology for the Earth, Development of an Advanced Refrigerant for Compression Heat Pumps; *RITE Report*; 1990−1995.

(6) Research Institute of Innovative Technology for the Earth, Survey of Alternative Methods and Molecular Design of New Candidate Compounds; *RITE Report*; 1996−2002.

(7) Intergovernmental Panel on Climate Change (IPCC), Third Assessment Report−Climate Change 2001: The Scientific Basis, Radiative Forcing of Climate Change; pp 388, Tables 6 and 7.

(8) Poling, B. E.; Prausnitz, J. M.; O'Connnell, J. P. *The Properties of Gases and Liquids*, 5th ed.; McGraw-Hill: New York, 2001.

(9) Maezawa, Y.; Sato, H.; Watanabe, K. Saturated Liquid Densities of HCFC 123 and HFC 134a. *J. Chem. Eng. Data* **1990**, *35*, 225−228.

(10) Baehr, H. D.; Tillner-Roth, R. Measurement and correlation of the vapor pressure of 1,1,1,2-tetrafluoroethane (R 134a) and of 1,1-difluoroethane (R 152a). *J. Chem. Thermodyn.* **1991**, *23*, 1063−1068.

(11) Japan Association of Refrigeration and Japan flon Gas Association. *Thermophysical Properties of Environmentally Acceptable Fluorocarbons, HFC-134a and HCFC-123*; Tokyo, Japan, 1991.

(12) Strom, K. H. U.; Gren, U. B. Liquid molar volume of CH_2FCF_3, CH_3CClF_2, and CH_3CHF_2 and the mixture of $CHFCl_2$+CH_3CClF_2 and CHF_2Cl+CH_3CHF_2. *J. Chem. Eng. Data* **1993**, *38*, 18−22.

(13) Aoyama, H.; Kishizawa, G.; Sato, H.; Watanabe, K. Vapor-liquid coexistence curves in the critical region and the critical temperatures and densities of 1,1,1,2-tetrafluoroethane (R-134a), 1,1,1-trifluoroethane (R-143a), and 1,1,1,2,3,3-hexafluoropropane (R-236ea). *J. Chem. Eng. Data* **1996**, *41*, 1046−1051.

(14) Fujiwara, K.; Nakamura, S.; Noguchi, M. Critical parameters and vapor pressure measurements for 1,1,1-trifluoroethane (R-143a). *J. Chem. Eng. Data* **1998**, *43*, 55−59.

(15) Mears, W. H.; Stahl, R. F.; Orfeo, S. R.; Shair, R. C.; Kells, L. F.; Thompson, W.; McCann, H. Thermodynamic properties of halogenated ethanes and ethylenes. *Ind. Eng. Chem.* **1955**, *47*, 1449−1454.

(16) Chae, H. B.; Schmidt, J. W.; Moldover, M. R. Alternative refrigerants R123a, R134, R141b, R142b, and R152a: critical temperature, refractive index, surface tension, and estimates of liquid, vapor and critical density. *J. Phys. Chem.* **1990**, *94*, 8840−8845.
(17) Yada, N.; Kumagai, K.; Tamatsu, T.; Sato, H.; Watanabe, K. Measurements of the thermodynamic properties of HCFC 142b. *J. Chem. Eng. Data* **1991**, *36*, 12−14.
(18) Tanikawa, S.; Tatoh, J.; Maezawa, Y.; Sato, H.; Watanabe, K. Vapor-liquid coexistence curve and critical parameters of 1-chloro-1,1-difluoroethane (HCFC-142b). *J. Chem. Eng. Data* **1992**, *37*, 74−76.
(19) Benning, A. F.; Mcharness, R. C. Thermodynamic properties of fluorochloromethanes and -ethanes. *Ind. Eng. Chem.* **1939**, *31*, 912−916.
(20) Wang, B.-H.; Adcock, J. L.; Mathur, S. B.; van Hook, W. A. Vapor pressures, liquid molar volumes, vapor non-idealities, and critical properties of some fluorinated ethers: $CF_3OCFEOCF_3$, CF_3OCF_2-CF_2H, c-$CF_2CF_2CF_2O$, CF_3OCF_2H, and CF_3OCH_3; and of CCl_3F and CF_2ClH. *J. Chem. Thermodyn.* **1991**, *23*, 699−710.
(21) Christou, G.; Young, C. L.; Svejda, P. Gas−liquid critical temperatures of binary mixtures of polar compounds + hydrocarbons or + other polar compounds. *Ber. Bunsen-Ges. Phys. Chem.* **1991**, *95*, 510−514.
(22) Tokuhashi, K.; Takahashi, A.; Kaise, M.; Kondo, S.; Sekiya, A.; Yamashita, S.; Ito, H. Rate constants for reactions of OH radicals with $CH_3OCF_2CHF_2$, $CHF_2OCH_2CF_2CHF_2$, $CHF_2OCH_2CF_2CF_3$, and $CF_3CH_2OCF_2CHF_2$ over the temperature range 250−430K. *J. Phys. Chem. A* **2000**, *104*, 1165−1170.
(23) Mogollon, E.; Kay, W. B.; Teja, A. S. Modified sealed tube method for the determination of critical temperature. *Ind. Eng. Chem. Fundam.* **1982**, *21*, 173−175.
(24) Smith, R. L., Jr.; Anselme, M.; Teja, A. S. The critical temperatures of isomeric pentanols and heptanols. *Fluid Phase Equilib.* **1986**, *31*, 161−170.
(25) Rosenthal, D. J.; Teja, A. S. Critical pressures and temperatures of isomeric alkanoles. *Ind. Eng. Chem. Res.* **1989**, *28*, 1693−1696.
(26) Quadri, S. K.; Khilar, K. C.; Kudchadker, A. P.; Patni, M. J. Measurement of the critical temperatures and critical pressures of some thermally stable or mildly unstable alkanols**.** *J. Chem. Thermodyn.* **1991**, *23*, 67−76.
(27) Murata, J.; Yamashita, S.; Akiyama, M.; Katayama, S.; Hiaki, T.; Sekiya, A. Vapor pressure of Hydrofluoroethers. *J. Chem. Eng. Data* **2002**, *47*, 911−915.

Received for review October 24, 2002. Accepted July 11, 2003. This work was financially supported by the New Energy and Industrial Technology Development Organization (NEDO).

JE0201976